www.czasopisma.pan.pl PAN POLSKA AKADEMIA NAUK www.journals.pan.pl

Arch. Metall. Mater. **62** (2017), 4, 2153-2163

DOI: 10.1515/amm-2017-0318

M. TENEROWICZ*#, M. SUŁOWSKI*#

THE EFFECT OF Mn CONTENT ON THE STRUCTURE AND PROPERTIES OF PM Mn STEELS

The aim of the study was to examine how a reduction of Mn content in PM steels will affect their plastic and strength properties. The results of mechanical, metallographic and fractography tests of sintered (PM) steels containing 1% and 2% Mn are reported and compared with those for 3% Mn PM steel. Höganäs iron powder grade NC 100.24, low-carbon ferromanganese Elkem and graphite powder grade C-UF were used as the starting powders. Powder mixes Fe-(1-2)%Mn-0.8%C were prepared in a Turbula mixer for 30 minutes. Following mixing, "dog bone" compacts were single pressed at 660 MPa, according to PN-EN ISO 2740 standard. Sintering of compacts was carried out in a laboratory tube furnace at 1120°C and 1250°C for 60 minutes in a mixture of 95%N_2 – 5%H_2 in a semi-closed container. Three types of heat treatment were then used: sinterhardening (cooling rate – 66°C/min), slow furnace cooling (cooling rate 3.5°C/min) and tempering at 200°C. The studies have shown a beneficial effect of the reduction of manganese on plastic properties (up to 7.96%), while maintaining fracture strengths (UTSs) comparable to those of steel with higher contents of manganese. Currently detailed studies of steel containing 1%Mn are conducted.

Keywords: sinterhardening, furnace cooling fractography, ductile fracture, brittle fracture, PM Mn steels

1. Introduction

In the traditional PM processes Cu, Ni and Mo as alloying elements are used [1]. Molybdenum is used because it increases strength and hardenability of sintered steel. Copper is characterized by similar physical properties to iron, but it is much more resistant to corrosion [2]. Nickel has a harmful influence on environment and is a cancerogenic and also an expensive element. Because of this, manganese can be used instead of nickel. Manganese can be added to the powder mixture as ferromanganese or electrolytic manganese powder. The main problem with using manganese in PM steels is its high affinity to oxygen. Due to the high vapour pressure of Mn at the sintering temperature, successful sintering of manganese steels was supposed to be possible due to a "self-cleaning" effect [3]. Manganese vapour reacts with oxygen during the sintering process and cleans the atmosphere inside the pores by creating fine dispersed oxides. This "purification" prevents specimen from further oxidation [4-7]. Another problem with manganese addition is inter-granular decohesion which can cause brittle fracture.

Stress-strain relationships in most PM steels, though not reaching the point of plastic instability, show limited plasticity, up to a few %. Failure is by crack propagation. Factors such as porosity and prior particle boundaries, as well as phases (ferrite, austenite, bainite, martensite, inclusions), influence initiation, coalescence and growth of microcracks and crack propagation [8]. All these microstructural features have characteristic fracture resistance and thus failure is frequently by combination of dimple rupture (evidence of local plasticity), cleavage, intergranular and interparticle failure micromechanisms.

To avoid the problem of low ductility in Mn steels, Cias [9] used a semi-closed container to create a special "micro-climate" around and within Fe-Mn-C compacts. Of several steels Cias et al [9-11] so investigated, noteworthy are 3-4% Mn, reported on by Sulowski and Ciaś [11,12]. They observed for 3% Mn content yield strengths above 400 MPa and tensile elongations up to 3.8%. It was thus thought of interest to continue these experiments by studying lower Mn contents.

2. Experimental

Höganäs iron powder grade NC 100.24, Elkem low-carbon ferromanganese (77% Mn, 1.3% C) (Eramet Norway Sauda) and graphite powder grade C-UF were used as the starting powders. From these mixtures with compositions of Fe-1%Mn-0.8%C and Fe-2%Mn-0.8%C were Turbula mixed for 30 minutes. Following mixing, green compacts according to PN-EN ISO 2740 standard were single-action pressed at 660 MPa. The average densities of green compacts were 6.68 g/cm^3 and 6.62 g/cm^3 for samples containing 1% and 2% Mn, respectively. To minimize friction, zinc stearate was used as a lubricant and was applied on the punches before pressing each sample. Following pressing, compacts were sintered at 1120°C and 1250°C for 60 minutes

* AGH UNIVERSITY OF SCIENCE AND TECHNOLOGY ,FACULTY OF METALS ENGINEERING AND INDUSTRIAL COMPUTER SCIENCE, AL. MICKIEWICZ 30, 30-059 KRAKÓW, POLAND

Corresponding author: tenerowi@agh.edu.pl, mtenerowicz@o2.pl

in the mixture of 95% N_2-5% H_2 in a semiclosed container, as used by Cias [9,10]. Three types of heat treatment after sintering were employed: sinterhardening (cooling rate 66°C/min), slow furnace cooling (cooling rate 3.5°C/min), and tempering at 200°C. Table 1 shows the designation, chemical composition and sintering variant of each sample, chosen from a batch of 10 or 5 samples. Additionally, for comparative analysis, data obtained for samples containing 3% Mn and 0.8% C (batches 3NCELATM_1 and 3NCELATM_2) are presented [13].

The steels were physically (green and as-sintered densities) and mechanically (tensile, 3-point bend and apparent hardness) tested at room temperature. Green and as-sintered (as-tempered) densities were calculated by the geometric method. Tensile testing was on a MTS 810 instrument at a cross-head speed of 1 mm/min. Tensile and bend strengths and hardness were calculated according to 10002-1 standard. TRS was measured using a ZD10-90 machine, following PN-EN 3325 standard. The load was applied to the surface on which the pressing punch contacted. Hardness was investigated on the microscale on an Innovatest machine using the Vickers method. Ten data points were taken on the length of the cross-sectional surface of the sample. Following mechanical tests, metallographic (LOM) and fracture investigations (SEM) were carried out using Leica DM 4000M and JEOL JSM 700F instruments, respectively. Samples were prepared according to the procedure described in [14].

TABLE 1

The designation, chemical composition and variants of sintering and heat treatment of Mn steels (representative sample chosen from batch of 10 or 5 samples)

Batch descriptions	No of sample	Chemical composition	Sintering variant
A1-A10	**A8**	1% Mn; 0.8% C	1120°C / SH / **temp**
A11-A15	**A14**		1120°C / SH / **NT**
A16-A20	**A16**		1120°C / **SC**
A21-A30	**A23**		1250°C / SH / **temp**
A31-A35	**A32**		1250°C / SH / **NT**
A36-A40	**A38**		1250°C / **SC**
M1-M10	**M6**	2% Mn: 0.8% C	1120°C / SH / **temp**
M11-M15	**M13**		1120°C / SH / **NT**
M16-M20	**M16**		1120°C / **SC**
M21-M30	**M22**		1250°C / SH / **temp**
M31-M35	**M35**		1250°C / SH / **NT**
M36-M40	**M39**		1250°C / **SC**
3NCELATM_1	**3N_1**	3% Mn; 0.8% C	1120°C / SH / **temp1**
3NCELATM_2	**3N_2**		1250°C / SH / **temp1**

SH – sinterhardening (cooling rate 66°C/min.), **SC** – slow cooling 3.5°C/min, tempering 200°C /air / 60 min, **temp1** – tempering 200°C / nitrogen / 60 min, **NT** – not tempered

3. Results

The results of mechanical properties of each batch of the investigated steels are summarised in Table 2. In Table 3 the results of mechanical properties of representative samples are presented.

It is seen in Table 3 that the highest tensile strength, UTS, was reported for sample 3N_2 – 715 MPa. The lowest value of UTS, 448 MPa, was recorded for sample M16. The highest elongation after tensile test, A, was recorded for sample A23 (7.96%), the smallest – for M35 (1.56%). The highest bend strength, TRS, was recorded for sample 3N_2 (1426 MPa). On the other hand, the lowest TRS was obtained for sample M13 (833 MPa). The highest average hardness was reported for sample M35 (319 HV 0.05) and the lowest value was achieved for sample 3N_1 (186 HV 30).

Generally, for the same processing history, as the Mn content decreased, so the yield stress, and plasticity increased, such that the fracture strengths (UTSs) did not vary significantly between 1-3 Mn contents, as illustrated in Figs. 1 and 2.

The microstructures of investigated steels are shown in Figures 3 and 4. Metallographic examination showed that microstructure of sintered steels containing 1% Mn consisted mainly of pearlite and ferrite; sometimes bainite (Fig. 3). This

TABLE 2

Mechanical properties of sintered Fe-(1-3)%Mn-0.8%C steels – mean values and standard deviations

No. of samples	Mean density, [g/cm^3]	Mean 0.2% offset stress, [MPa]	Mean UTS, [MPa]	Mean TRS, [MPa]	A, [%]
A1-A10	6.70 ± 0.02	257 ± 6	603 ± 25	1034 ± 87	6.7 ± 0.6
A11-A15	6.69 ± 0.02	261 ± 4	597 ± 17	971 ± 70	6.9 ± 1.5
A16-A20	6.70 ± 0.01	261 ± 3	551 ± 12	907 ± 73	6.3 ± 0.7
A21-A30	6.69 ± 0.02	260 ± 15	690 ± 56	1211 ± 96	7.7 ± 0.8
A31-A35	6.67 ± 0.03	248 ± 25	678 ± 43	1188 ± 57	7.8 ± 1.5
A36-A40	6.64 ± 0.03	287 ± 62	622 ± 45	1216 ± 110	5.8 ± 1.5
M1-M10	6.63 ± 0.05	301 ± 9	578 ± 19	847 ± 71	3.4 ± 0.4
M11-M15	6.66 ± 0.01	295 ± 8	533 ± 28	841 ± 55	2.8 ± 0.3
M16-M20	6.65 ± 0.02	295 ± 6	448 ± 26	843 ± 50	4.2 ± 0.5
M21-M30	6.64 ± 0.05	318 ± 11	611 ± 53	1035 ± 100	3.8 ± 0.7
M31-M35	6.64 ± 0.02	327 ± 27	498 ± 52	1078 ± 111	2.9 ± 0.8
M36-M40	6.65 ± 0.03	311 ± 7	644 ± 14	1018 ± 41	4.7 ± 0.4
3NCELATM_1	6.82±0.07	420± 15	657 ± 30	1234 ± 115	1.82 ± 0.17
3NCELATM_2	6.83±0.10	451 ± 20	724 ± 68	1419 ± 114	1.67 ± 0.25

TABLE 3

Mechanical properties of representative sintered Fe-(1-3)% Mn-0.8% C steels

No. of samples	Density, [g/cm^3]	0.2% offset stress, [MPa]	UTS, [MPa]	TRS, [MPa]	A, [%]	Hardness HV 0.05
A8	6.71	259	623	1023	7.48	311
A14	6.70	267	609	981	6.97	209
A16	6.72	253	545	916	5.79	235
A23	6.71	266	708	1199	7.96	231
A32	6.66	233	639	1186	7.10	272
A38	6.61	261	663	1226	6.77	230
M6	6.66	302	578	837	3.91	256
M13	6.66	291	533	833	2.56	254
M16	6.65	257	448	837	3.44	224
M22	6.51	326	611	1046	3.69	258
M35	6.67	355	498	1058	1.56	319
M39	6.63	303	644	1015	5.47	253
3N_1	6.89	410	660	1230	1.87	186*
3N_2	6.93	425	715	1341	1.60	266*

*) HV 30

observation corresponds to average $R_{0.2}$ in the range from 248 to 287 MPa for this steel, depending on the sintering temperature and post sintering heat treatment. With manganese increasing to 2%, bainite and occasionally martensite were observed (bainitic-martensitic structure) – average $R_{0.2}$ is in the range from 295 to 327 MPa (Table 2). Further increase of Mn content resulted in the creation of more martensite in the structure (martensitic-bainitic structure).

Figures 5-10 present the fractures of Fe-1%Mn-0.8%C sintered at both 1120 and 1250ºC. In Fig. 5 fractography of sample A8, produced with 1120ºC/SH/tempering regime, is presented. Figure 5a presents a large quantity of ductile fracture with transgranular dimples (Fig. 5b).

Figure 6 presents fracture of A14 sample, which was produced using 1120°C/SH/NT variant. In the fracture of this steel undissolved particles of FeMn (Fig. 7a) and small areas of cleavage (Fig. 6b) are visible.

Figure 7 presents the fracture of A16 which was produced using 1120°C/SC variant. In the right corner of Fig. 7a cleavage appears. Figure 7b presents the area of brittle fracture of sample A16.

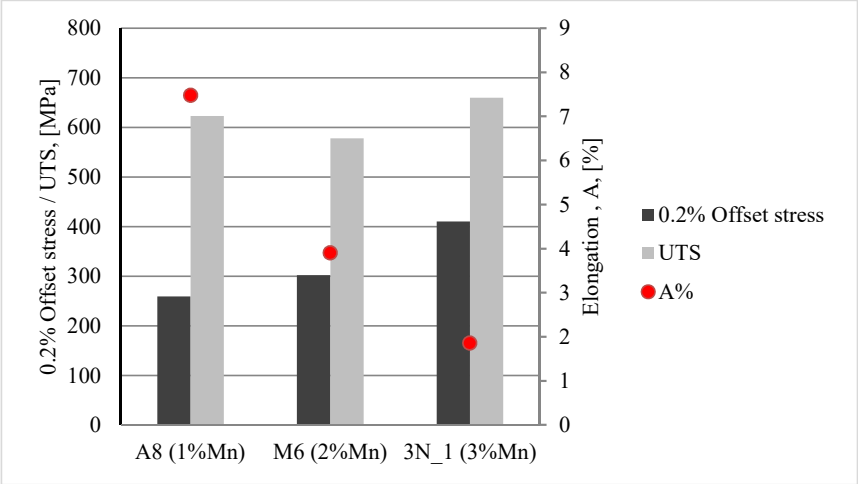

Fig. 1. Mechanical properties of 1-3Mn PM steels vs. Mn concentration– sintering temperature 1120°C

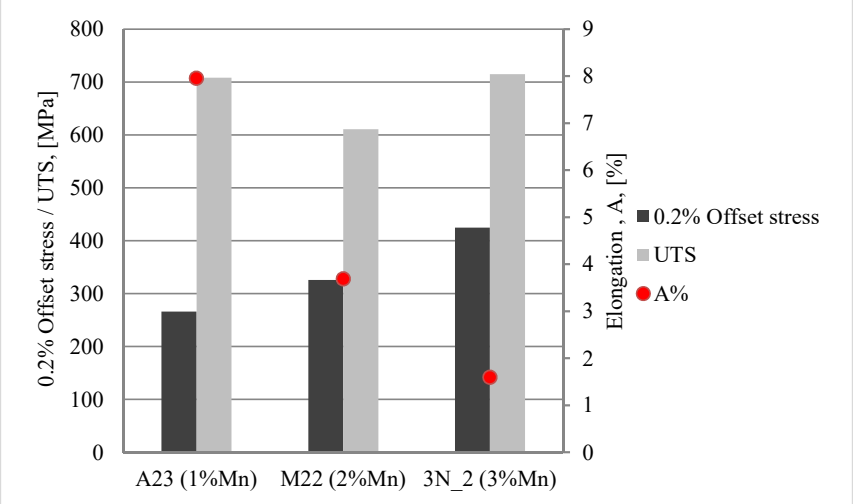

Fig. 2. Mechanical properties of 1-3Mn PM steels vs. Mn concentration– sintering temperature 1250°C

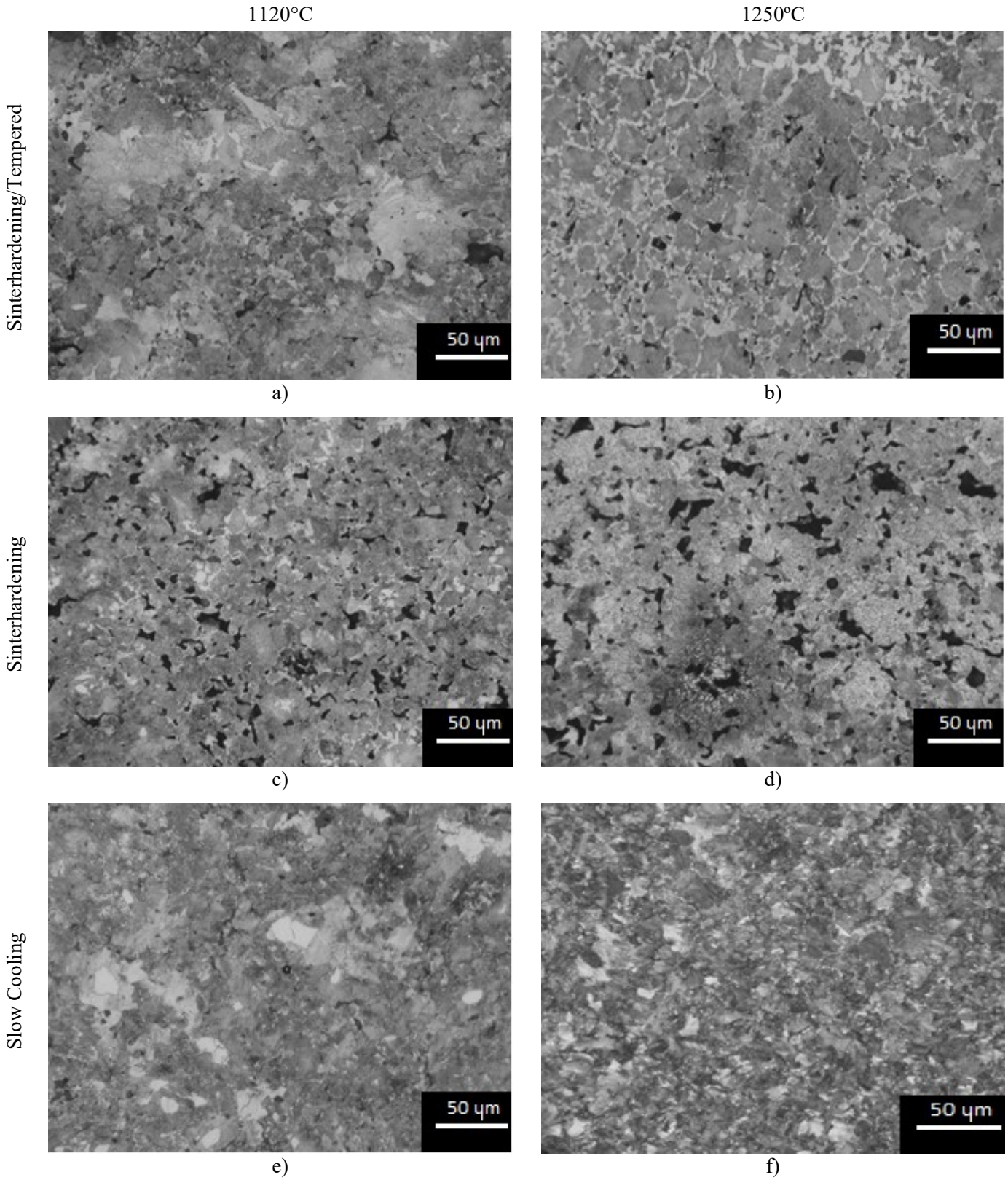

Fig. 3. Photomicrographs of Fe-1%Mn-0.8%C PM steel: a) 1120°C/SH/temp, b) 1250°C/SH/temp, c) 1120°C/SH/NT, d) 1250°C/SH/NT, e) 1120°C/SC, f) 1250°C/SC

Figure 8 shows the fracture of sample A23, produced using 1250°C/SH/tempered route. In this steel interparticle/interface fracture, shallow dimples and some small cleavage in bainite was observed (Fig. 8a). In Figure 8b interparticle fracture in fine pearlite and large oxide particles were noticed.

Figure 9 presents the fracture of sample A32 which was produced using 1250°C/SH/NT variant. In Fig. 9a the area with intergranular failure and some cleavage is shown. Figure 9b presents a "river pattern" which is characteristic of brittle fracture.

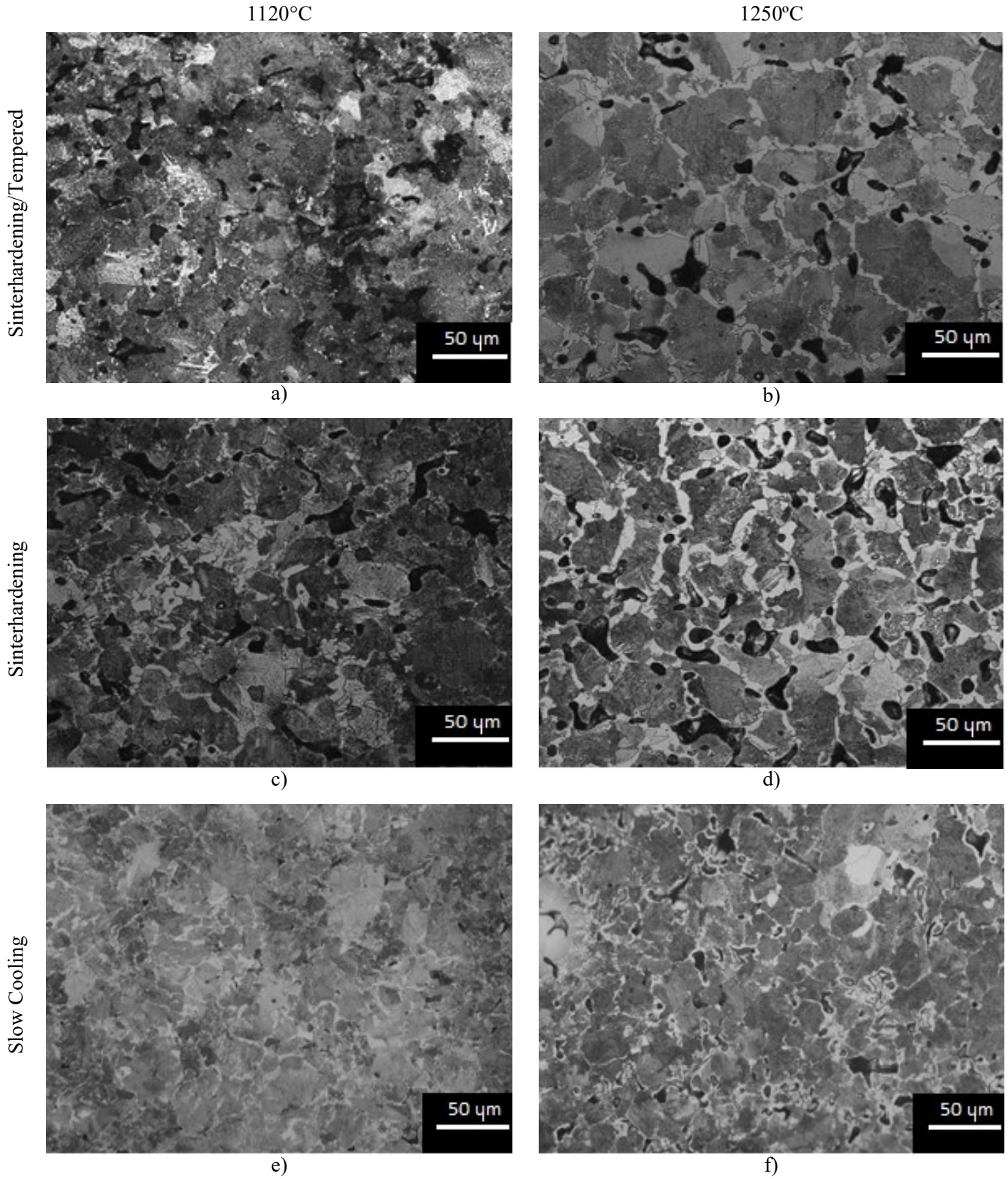

Fig. 4. Photomicrographs of Fe-2%Mn-0.8%C PM steel; a) 1120°C/SH/temp, b) 1250°C/SH/temp, c) 1120°C/SH/NT, d) 1250°C/SH/NT, e) 1120°C/SC, f) 1250°C/SC

Figure 10 presents the fracture of sample A38, produced using 1250°C/SC variant. It is characterized by interparticle/interface failure and some cleavage in bainite (Fig. 10a), and by interface failure/shallow dimples, some cleavage and some failure in pearlite along cementite lamellae (Fig. 10b).

Figures 11-16 present the fractures of Fe-2%Mn-0.8%C sintered at both 1120 and 1250°C. Figure 11 presents the fracture of sample M6 which was produced using 1120ºC/SH/tempered route. In Fig. 11a interparticle failure with shallow dimples initiated with oxide particles is shown, also some cleavage and

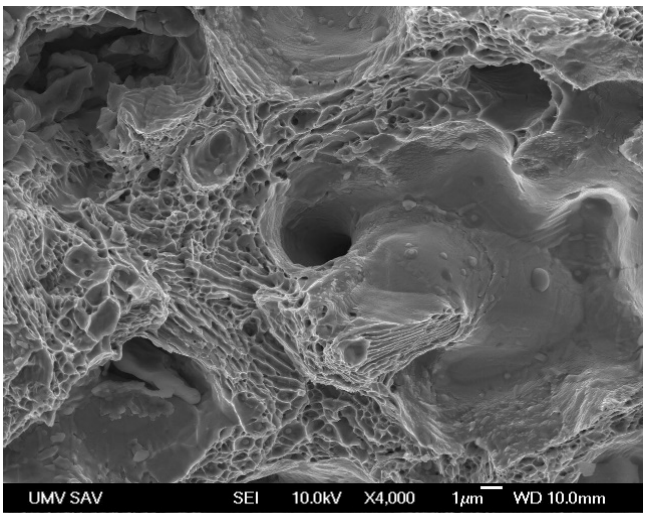

a)

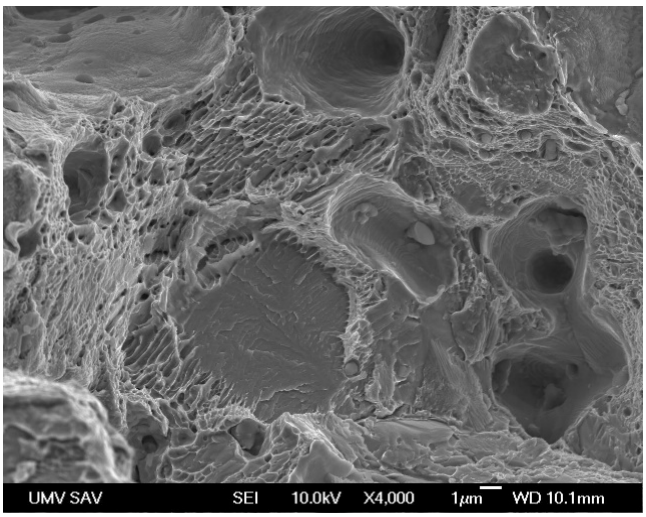

b)

Fig. 5. Fractography of sample A8

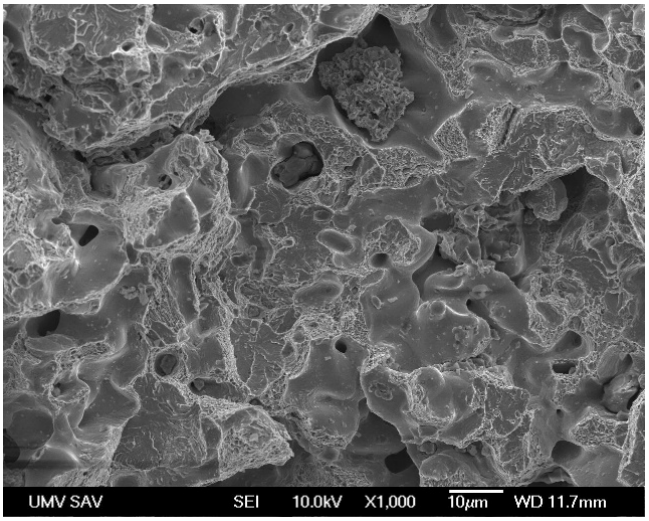

a)

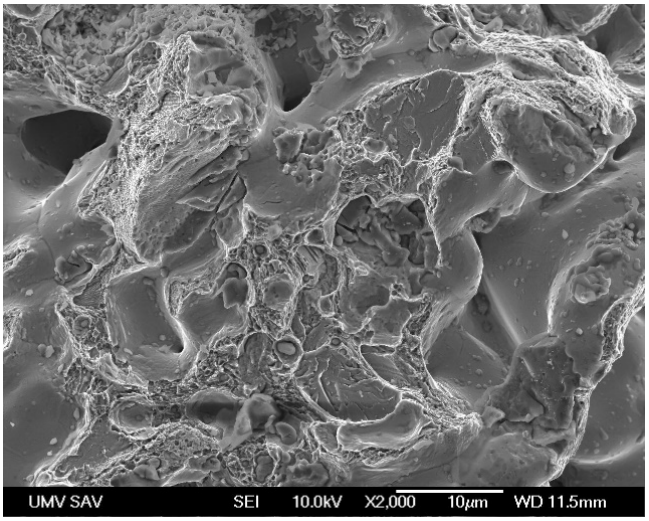

b)

Fig. 6. Fractography of sample A14

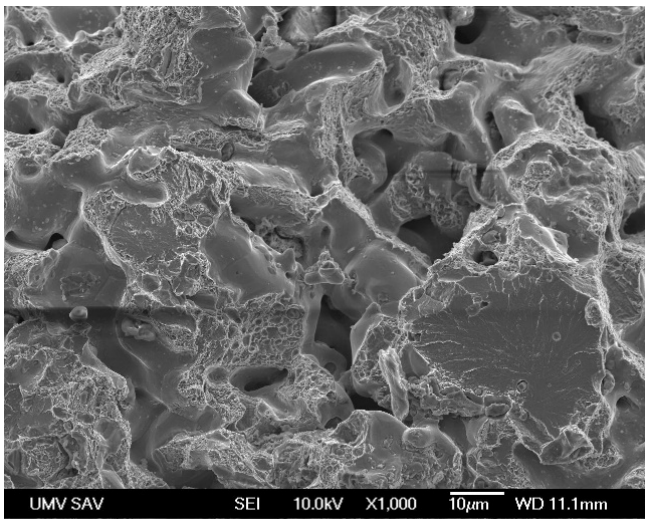

a)

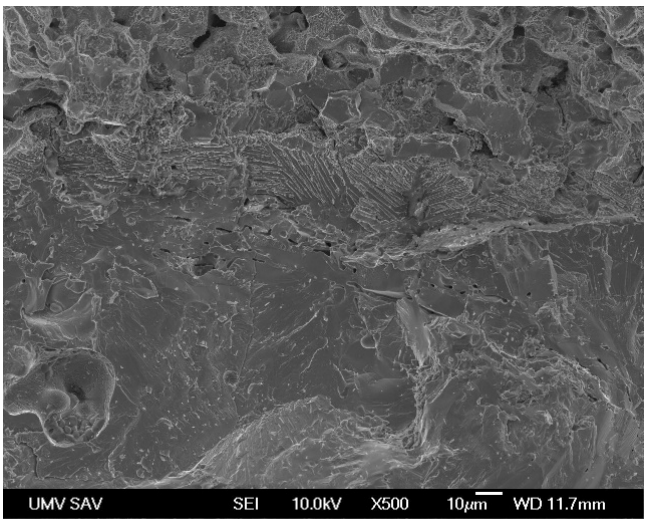

b)

Fig. 7. Fractography of sample A16

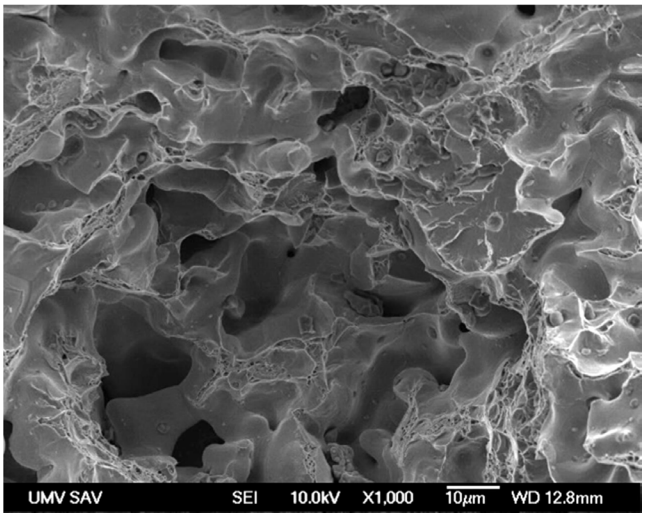

a)

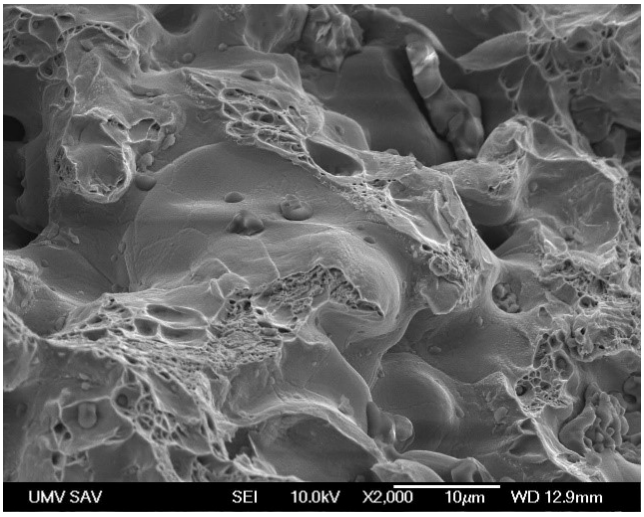

b)

Fig. 8. Fractography of sample A23

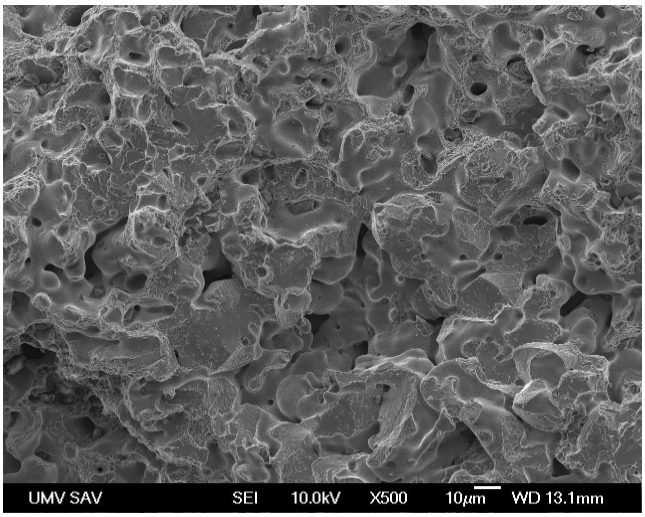

a)

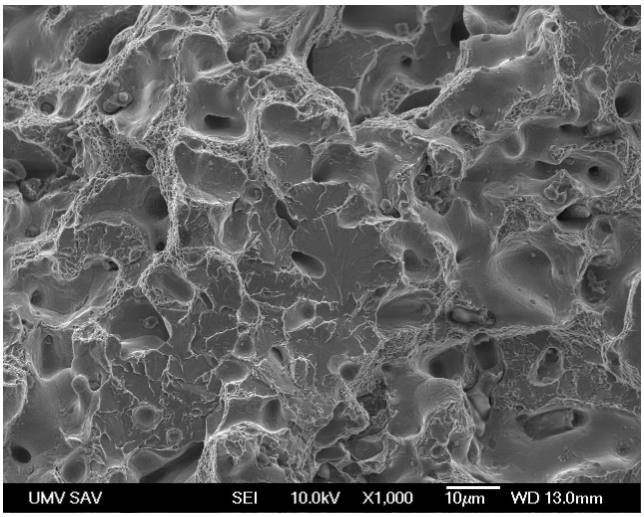

b)

Fig. 9. Fractography of sample A32

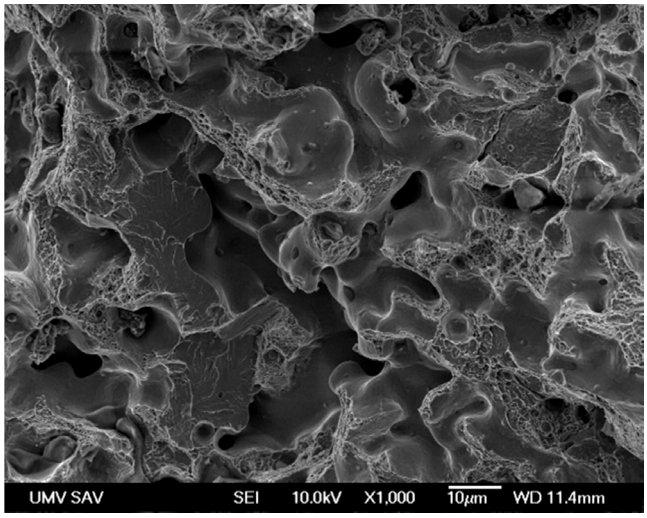

a)

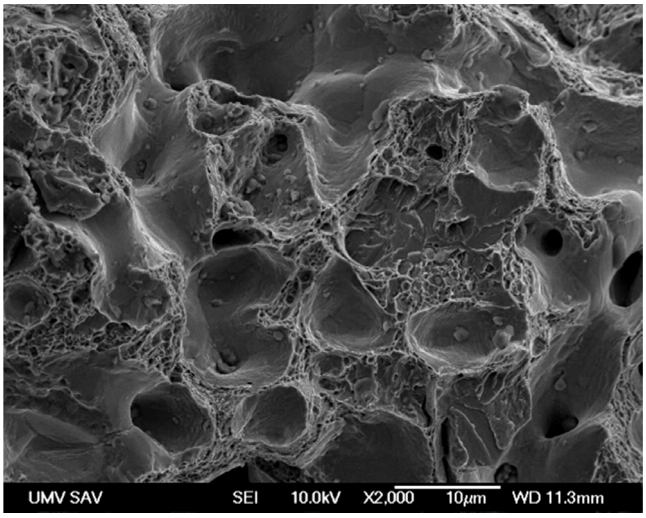

b)

Fig. 10. Fractography of sample A38

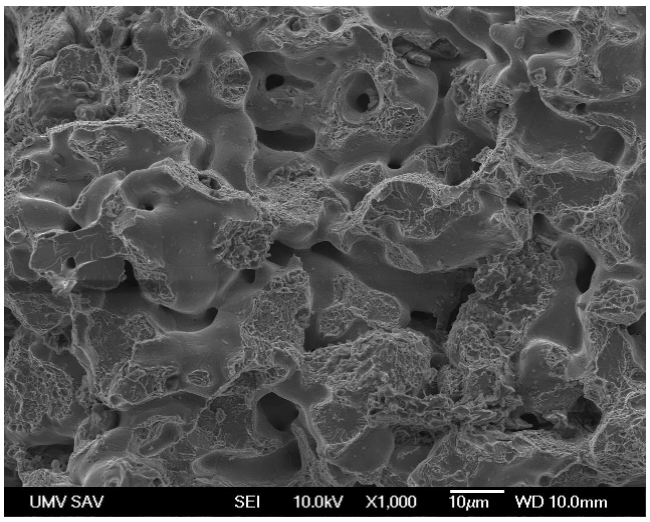

a)

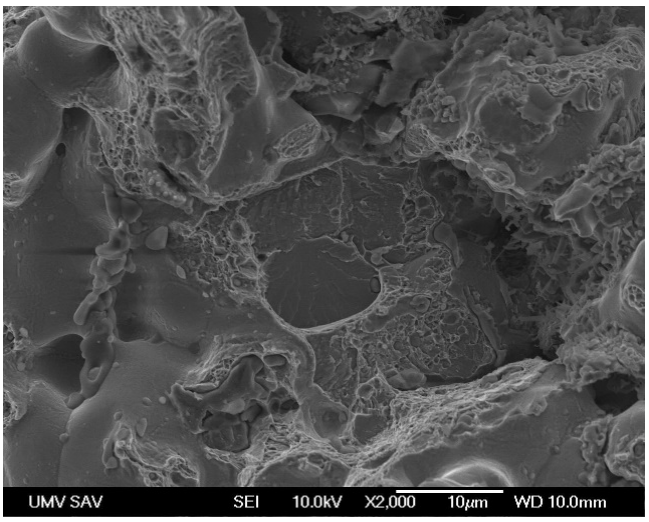

b)

Fig. 11. Fractography of sample M6

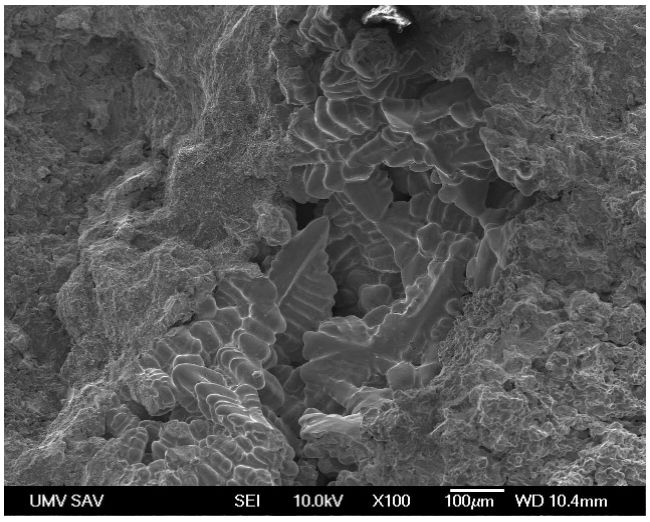

a)

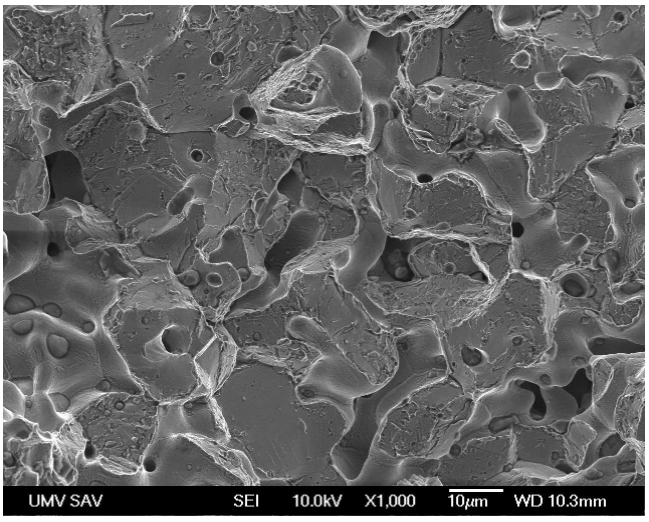

b)

Fig. 12. Fractography of sample M13

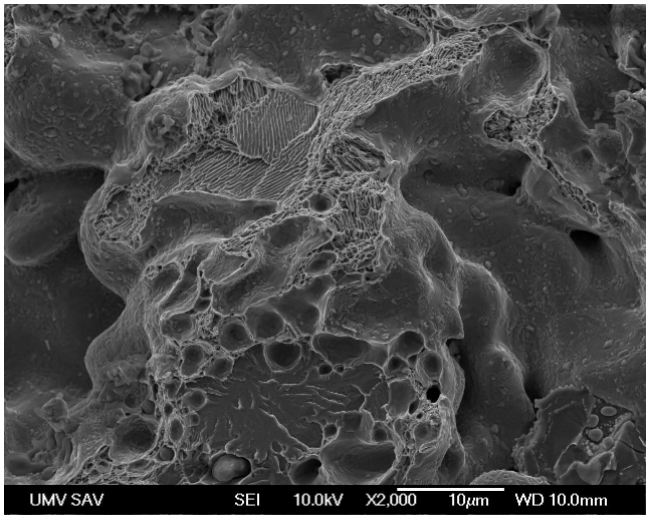

a)

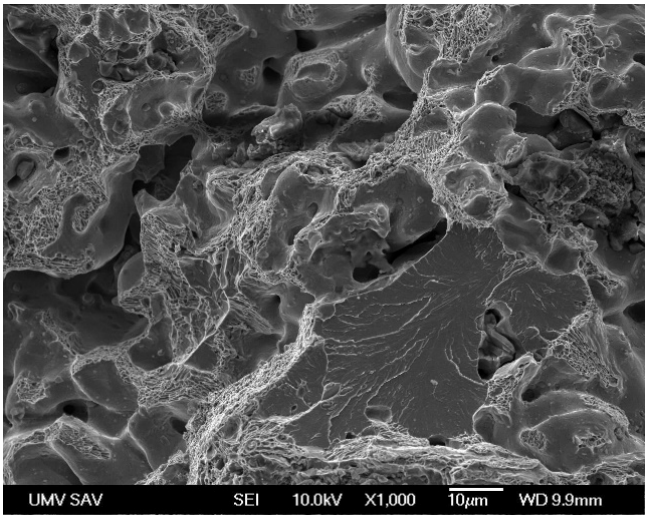

b)

Fig. 13. Fractography of sample M16

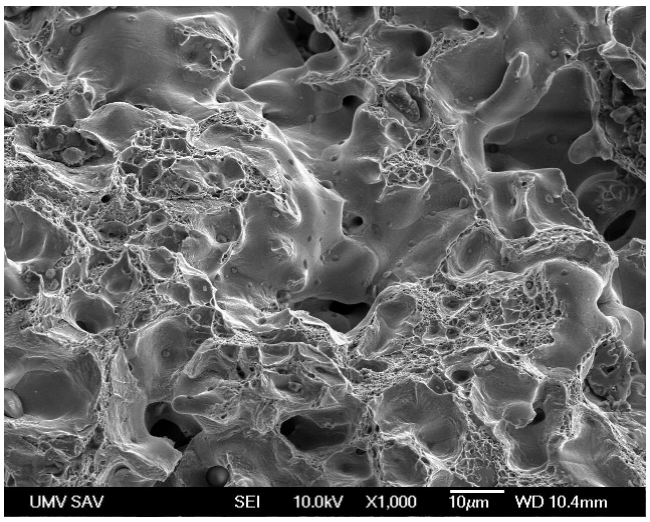

a)

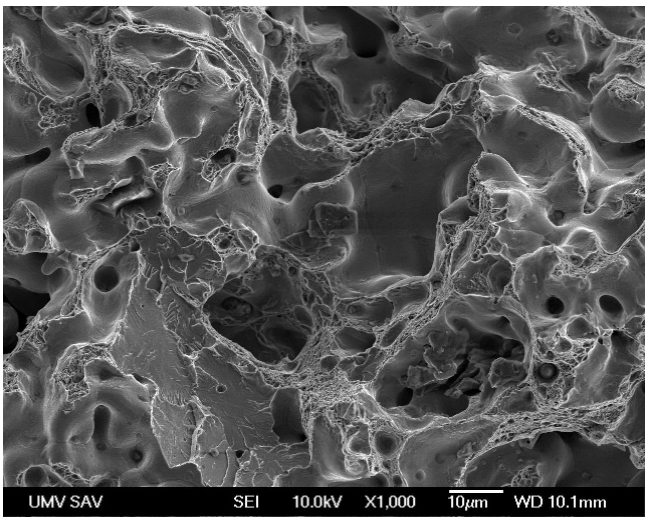

b)

Fig. 14. Fractography of sample M22

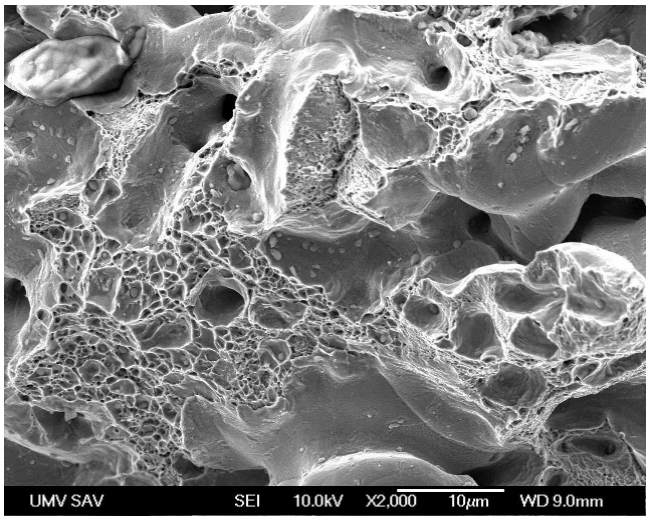

a)

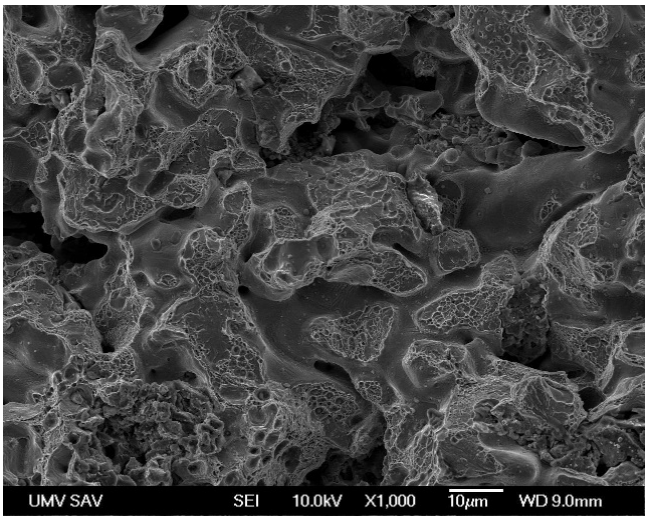

b)

Fig. 15. Fractography of sample M35

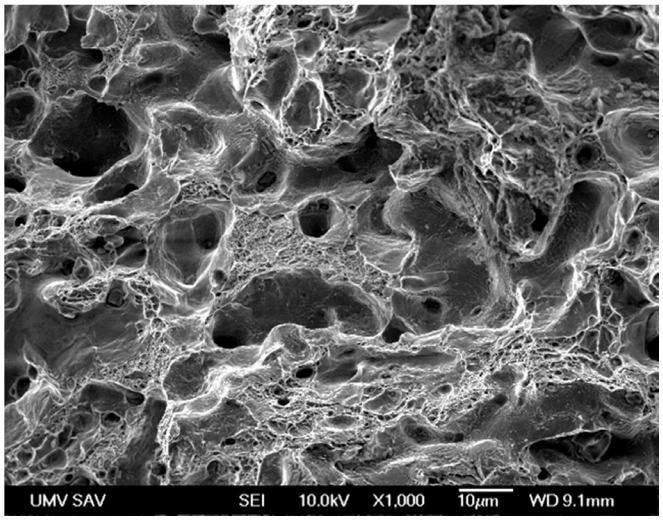

a)

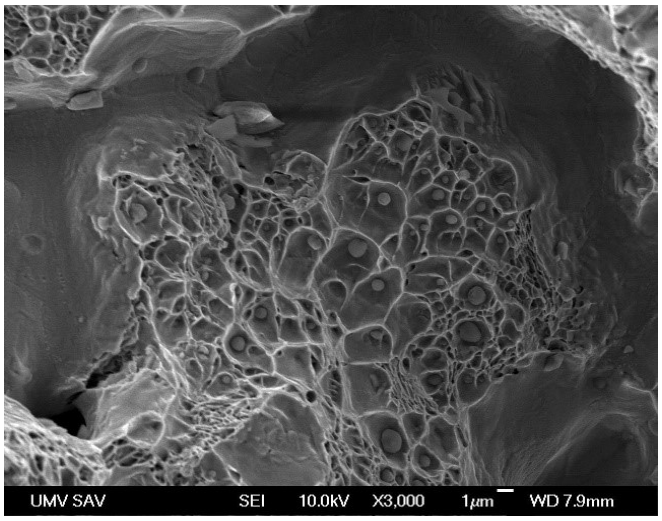

b)

Fig. 16. Fractography of sample M39

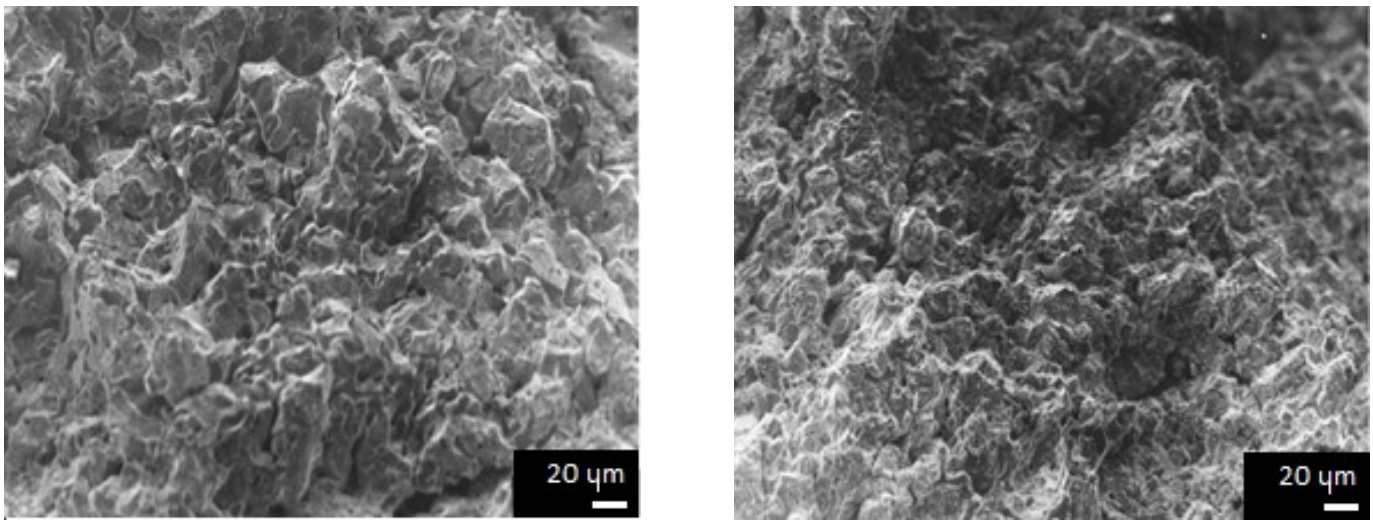

a) b)

Fig. 17. Fractography of Fe-3% Mn-0.8% C; a) Brittle fracture of 3N_1 sample, sintered at 1120ºC, b) ductile fracture of 3N_2 sample, sintered at 125°C [13]

many oxides. In the centre of Fig. 11b, an undissolved FeMn particle was noticed. The area around FeMn particle consists of many oxides.

Figure 12 presents the fracture of M13, produced using 1120°C/SH/NT variant. Fig. 12a presents a defect-solidified eutectic phase. This variant exhibits intergranular failure (Fig. 12b).

Fig. 13 presents the fracture of M16 which was produced using 1120°C/SC conditions. Failure in pearlite (also along cementite lamellae) – Fig. 13a, and some cleavage in bainite. In Fig. 13b failure in pearlite along cementite lamellae is also presented.

In Fig. 14 fracture of sample M22 is presented. This steel was produced using 1250°C/SH/tempered variant. Local plastic flow had occurred (relatively high strength particle connection) – Fig. 14a; also river line patterns were observed (Fig. 14b).

In Fig. 15 the fracture of sample M35 (1250ºC/SH/NT) is presented. It is characterised by ductile fracture (dimples) – Fig. 15a. Large amount of oxides was present (Fig. 15b).

Figure 16 presents the fracture of sample M39, produced using 1250°C/SC conditions. Relatively strong local plastic flow was observed in Fig. 16a. Figure 16b presents a large concentration of oxides in dimples.

Figure 17 presents brittle and ductile fracture of Fe-2%Mn-0.8%C PM steels (samples 3N_1 and 3N_2), after sintering at 1120°C and 1250°C, respectively. In Figure 17a brittle fracture was observed (transgranular cleavage), Figure 17b present transparticle ductile fracture of sample 3N_2.

The prevalent fracture micromechanisms were interparticle/interface failure – fine and coarse shallow dimples initiated by oxide particles, failure in pearlite (elongated dimples or failure along cementite lamellae), and some cleavage in bainite. In areas surrounding the previous FeMn particles small intergranular facets were also observed. The remnants of FeMn particles are often observed (large pores with FeMn).

4. Discussion

The mechanical properties data are illustrated in Figs. 1 and 2. Considering properties of 1 and 2% Mn alloys, and primarily $R_{0.2}$, noticeable are the relatively small differences between different heat treatments after the same sintering temperature. Many results (e.g. all of $R_{0.2}$ for 1% Mn variants) are within the experimental error. There is the expected increase in $R_{0.2}$ after sintering at 1250°C, with a small decrease in plasticity, but still at ~3% strain. The 3% Mn data show further increase in strength, due to martensite, and decrease in plasticity. The fracture strength, UTS, of 1-3% Mn specimens did not vary greatly between all Mn contents.

High plasticity of slow cooled 3-4% PM Mn steels has been already reported by Sulowski and Ciaś [11,12]. They showed that decreasing the cooling rate to 3.5°C/min (furnace cooling) in some cases increased fracture strengths (UTSs) by a factor up to ~2 and tensile elongation up to 3.8% [12]. In our experiments with 1-2 Mn steels it was noted that the ductility of the steels was even higher: elongation up to ~8%. It is our hypothesis that the increase in plasticity is related to sintering in a semi-closed container.

This phenomenon was discussed in detail by Cias [15] for Fe-3%Cr0.5%Mo-0.6%C steel similarly processed. He considered the microclimate within the pores, where reduction is favoured due to more intensive carbothermic processes. He related his observations to those of Kabatova et al. [16,17], who found that tensile failure was associated with nucleation of microcracks, their growth and coalescence. They reported that microcrack coalescence was associated with easy paths for (micro)crack growth, principally prior particle boundaries linking pores. To improve ductility/increase fracture strength, (micro) cracking needs to be made more difficult. Conversely, reduced ductility of Cr and Mn sintered steels has been associated, e.g. by Hryha et al. [18] and Hrubovcakova et al. [19], with bound-

ary contamination. It is therefore suggested that sintering in a semi-closed container results in improved cleanliness of such boundaries, making (micro)cracking more difficult and enabling further plastic flow before fracture in our steels.

5. Conclusions

1. The microstructure of 1% and 2% Mn sintered steels consisted mainly of ferrite and pearlite.
2. The high plasticity and fracture strengths (UTSs) are attributed to sintering in a semi-closed container.
3. With a manganese content of 1% good mechanical properties were obtained.
4. In the case of steels containing 3%Mn, chemical composition and manufacturing conditions contributed to an increase in strength and a decrease in plasticity.
5. Fractography investigations showed that when pearlite is present, ductile fracture was observed.
6. With increase of the amount of manganese and hence the appearance of bainite in the structure, the number of brittle facets increases (cleavage in bainite).
7. The results indicate the need for further research of sintered steel containing 1%Mn, especially slow cooled.

Acknowledgments

The financial support of the Ministry of Science and Higher Education under AGH contract no 5.72.110.420 is acknowledged.
The authors would like to thank Dr. E. Dudrova, SAS, Kosice, for her help and important comments. The authors would also like to thank Prof. A.S. Wronski for his content-related comments and editing this text.

REFERENCES

[1] E. Hryha, E. Dudrova, L. Nyborg, Metall. Mater. Trans. A **41A**, 2880 (2010).
[2] http://stalesia.com/index.php?/3/faq/pierwiastki_stopowe_w_stali, (02.09.2016).
[3] A. Šalak, M. Selecká, DOI: 10.1007/978-1-907343-75-9, Cambridge International Science Publishing, 2012.
[4] E. Hryha, L. Nyborg, E. Dudrova, S. Bengtsson, Euro PM2009-Sintered Steels 1- Composition 1, 17-22.
[5] E. Hryha, Fundamental Study of Mn Containing PM Steels with Alloying Methods of both Premix and Prealloy, PhD Thesis, IMR SAS, Kosice, 2007.
[6] E. Hryha, Powder Metall. Prog. **8** (2), 109-114 (2008).
[7] E. Hryha, Mat. Sci. Forum 534-536, 761-764 (2007).
[8] E. Dudrova, Powder Metall. **59** (2), 148-167 (2016).
[9] A. Cias, S.C. Mitchell, K. Pilch, H. Cias, M. Sulowski, A.S. Wronski, Powder Metall. **46** (2),165-170 (2003).
[10] A. Cias, Kraków, AGH Uczelniane Wydawnictwa Naukowo-Dydaktyczne (2004).
[11] M. Sułowski, A. Ciaś, Archives of Metallurgy and Materials **49** (1), 55-72 (2004).
[12] M. Sułowski, Archives of Metallurgy and Material **49** (3), 641-670. (2004).
[13] M. Sułowski, The Structure and Mechanical Properties of Structural Sintered Fe-Mn-C Steels, Ph. D. Thesis, AGH UST, Cracow.
[14] L. Bjerregaard, K. Geels, B. Ottesen, Metalog Guide, Struers A/S, (2002).
[15] A. Cia, Powder Metall. **56** (3), 231-238, (2013).
[16] M. Kabatova, E. Dudrova and A.S. Wronski, Powder Metall. **49** (4), 363-368 (2006).
[17] M. Kabatova, E. Dudrova and A. S. Wronski, Powder Metall. Prog. **5** (3), 185-193 (2005).
[18] E. Hryha, L. Cajkova and E. Dudrova, Powder Metall. Prog. **7** (4), 181-197 (2007).
[19] M. Hrubovcakova, E. Dudrova and J. Harvanova, Powder Metall. Prog. **11** (1-2), 115-123 (2011).